Table 1. Values of n and the maximum error of the heat transfer correlation equation over the whole range of velocity ratio

Range of Pr	Values of n	Maximum error (%)
$0.01 \leqslant Pr \leqslant 0.1$	0.76	5.7
$0.1 \leqslant Pr \leqslant 0.7$	0.84	6.5
$0.7 \leqslant Pr \leqslant 7$	0.97	5.2
$7 \leqslant Pr \leqslant 10\,000$	1.02	1.4

For the case of a reverse moving surface, Fig. 4(b) shows that $Nu/Re_x^{1/2}$ decreases as ξ increases. The decrease of the Nusselt number is due to the back flow of hot fluid from the down-stream.

3.4. *Correlation equations of heat transfer*

A correlation equation of the local Nusselt number for any velocity ratio is developed as

$$\left(\frac{Nu}{\lambda}\right)^n = \left[(1-\xi)\frac{Nu_B}{(\omega Re_x)^{1/2}}\right]^n + \left[\xi\frac{Nu_S}{(\sigma Re_W)^{1/2}}\right]^n. \quad (27)$$

This correlation can be rewritten as

$$\frac{Nu}{(\omega Re_x)^{1/2}} = (1-\xi)^{1/2}\left[\left(\frac{Nu_B}{(\omega Re_x)^{1/2}}\right)^n + \left(\frac{\xi}{1-\xi}\frac{Nu_S}{(\sigma Re_W)^{1/2}}\right)^n\right]^{1/n} \quad (28)$$

where $Nu_B/(\omega Re_x)^{1/2}$ for the special case of the Blasius problem ($\gamma = 0$) can be estimated from the correlation in ref. [7]:

$$Nu_B/Re_x^{1/2} = 0.3386Pr^{1/2}/(0.0526+0.1121\,Pr^{1/2}+Pr)^{1/6}. \quad (29)$$

The maximum error of this correlation does not exceed 1.4% for $0.001 \leqslant Pr \leqslant \infty$. While $Nu_S/(\sigma Re_W)^{1/2}$ for the special case of the Sakiadis problem ($\gamma = 1$) can be predicted by the present correlation equation

$$Nu_S/Re_W^{1/2} = 0.5642Pr^{1/2}/(0.4621+0.1395Pr^{1/2}+Pr)^{1/2}. \quad (30)$$

The maximum error of this correlation is less than 1% for $0.01 \leqslant Pr \leqslant 10\,000$.

Appropriate values of the exponent n in the correlation equations (27) and (28) for different Pr are presented in Table 1. Predictions of heat transfer from the correlation coincide satisfactorily with the numerical results, as indicated in this table.

4. CONCLUSIONS

This paper studied the general convection problem of a continuous moving surface in a flowing fluid by introducing novel transformation variables and parameters of velocity ratio. For the case of a plane surface moving in parallel to a free stream, very accurate similarity solutions and correlation equations for predicting the wall friction and heat transfer rate have been obtained for any ratio of surface velocity and free stream velocity over the range of $0.01 \leqslant Pr \leqslant 10\,000$. The case of a surface moving in the reverse direction of the free stream has also been analyzed. Velocity and temperature profiles have been presented to show the effects of the relative motion of the plane surface and the free stream. The developed analysis method can be applied to the mixed convection problems and many others.

Acknowledgements—This work was supported by a grant NSC80-0402-E008-08 from the National Science Council of R.O.C.

REFERENCES

1. H. Blasius, Grenzschichten in Flussig-keiten mit kleiner Reibung, *Z. Math. Phys.* **56**, 1–37 (1908).
2. H. T. Lin and L. K. Lin, Similarity solutions for laminar forced convection heat transfer from wedges to fluids of any Prandtl number, *Int. J. Heat Mass Transfer* **30**, 1111–1118 (1987).
3. B. C. Sakiadis, Boundary-layer behavior on continuous moving surface—Parts 1 and 2, *A.I.Ch.E. Jl* **7**, 26–28, 221–225 (1961).
4. F. Tsou, E. M. Sparrow and R. Goldstein, Flow and heat transfer in the boundary layer on a continuous moving surface, *Int. J. Heat Mass Transfer* **10**, 219–235 (1967).
5. T. A. Abdelhafez, Skin friction and heat transfer on a continuous flat surface moving in a parallel free stream, *Int. J. Heat Mass Transfer* **28**, 1234–1237 (1985).
6. P. R. Chappidi and F. S. Gunnerson, Analysis of heat and momentum transport along a moving surface, *Int. J. Heat Mass Transfer* **32**, 1383–1386 (1989).
7. H. T. Lin, W. S. Yu and C. C. Chen, Comprehensive correlations for laminar mixed convection on vertical and horizontal flat plates, *Wärme- und Stoffübertragung* **25**, 353–359 (1990).

Int. J. Heat Mass Transfer. Vol. 37, No. 2, pp. 336–340, 1994
Printed in Great Britain

0017-9310/94 $6.00 + 0.00

Thermal entrance length and Nusselt numbers in coiled tubes

NARASIMHA ACHARYA,† MIHIR SEN† and HSUEH-CHIA CHANG‡

† Department of Aerospace and Mechanical Engineering and ‡ Department of Chemical Engineering, University of Notre Dame, Notre Dame, IN 46556, U.S.A.

(*Received* 8 *June* 1993 *and in final form* 7 *July* 1993)

INTRODUCTION

SECONDARY flow in coiled tubes, generated as a result of tube curvature, significantly increases heat transfer as compared to flow in straight tubes. In straight tubes the peripherally averaged Nusselt number, $\langle Nu\rangle_\phi$, is a maximum at the tube inlet, decreases monotonically in the downstream direction, and asymptotes to a fully developed value. In coiled tubes on the other hand, $\langle Nu\rangle_\phi$ undergoes spatial oscillations before settling down to a fully developed value. Numerical calculations of this phenomenon have been carried out by Dravid *et al.* [1], Tarbell and Samuels [2], Patankar *et al.* [3], Akiyama and Cheng [4] and Janssen and Hoogendoorn [5]. There is also some experimental evidence in the observed spatial wall temperature oscillations reported by Dravid *et*

NOMENCLATURE

a	tube radius
De	Dean number, $Re\sqrt{(a/R)}$
Nu	Nusselt number based on tube diameter
Pe	Peclet number, $Re\,Pr$
Pr	Prandtl number
R	coil radius
r	dimensionless radial coordinate
Re	Reynolds number based on tube diameter
T	dimensionless fluid temperature, $(T^* - T^*_{wall})/(T^*_{inlet} - T^*_{wall})$
T^*	dimensional fluid temperature
u, v, w	dimensional radial, angular and axial velocity components
z	dimensionless axial coordinate
z_{min}	z at minimum Nusselt number
z_{max}	z at maximum Nusselt number
z_e	dimensionless entrance length.

Greek symbols

δ	radius ratio, a/R
δ_t	thickness of thermal boundary layer
ε	eccentricity
ϕ	angular coordinate.

Other symbols

$\langle\ \rangle_\phi$	average over angular coordinate ϕ.

al. [1]. However, the local increase in $\langle Nu\rangle_\phi$ is as yet unexplained. It is our purpose to clarify the mechanism responsible for the variation in the entrance Nusselt number and to present correlations for characteristic distances involved and Nusselt numbers.

We consider steady, laminar, constant property flow of a Newtonian fluid in loosely coiled tubes of circular cross-section with negligible viscous dissipation. The flow is considered thermally developing but hydrodynamically fully developed. Inlet temperature is uniform and the wall is at a constant but different temperature. An (r, ϕ, z) coordinate system is employed where z is distance along the axis of the tube measured from the inlet, and (r, ϕ) are polar coordinates at that z section. The characteristic length and velocity used for nondimensionalization are tube radius and average axial velocity respectively.

The governing equations are parabolized by neglecting axial gradient terms in the momentum and energy equations. A finite-volume numerical scheme is used to solve the equations. The code is validated by comparing calculated friction factors and Nusselt numbers against known theoretical and experimental results [6]. Computed $\langle Nu\rangle_\phi$ in the thermal entrance region is shown in Fig. 1 for various Reynolds numbers, Re, and given values of Prandtl number, Pr, and radius ratio, δ. The oscillatory behavior of $\langle Nu\rangle_\phi$ in the entrance region is evident in these results. There are four regions, marked 1–4, that can be identified in the figure.

Detailed numerical results show that a uniform temperature field at the inlet is initially cooled at the wall almost axisymmetrically such that a thin thermal boundary layer develops around a hot zone in the middle of the tube. This is region 1 where the temperature field is similar to that in a straight tube. In a straight tube, however, the thermal boundary layer would continue to grow axisymmetrically downstream with the Nusselt number decreasing monotonically. For a coiled tube, secondary flow pushes the hot fluid away from the center and towards the outer wall of the tube. This happens in region 2 as the computed isotherms shown in Fig. 2 indicate. Loss of axisymmetry of the isotherms leads to an increase in Nusselt number. In physical terms this can be related to heat conduction between two eccentric cylinders kept at different temperatures (see, for example, [7]). As the eccentricity is increased, there is some variation of local heat transfer around the periphery; but for small eccentricities the average Nusselt number increases as the square of the eccentricity. In coiled tubes there is also a circumferential variation in local Nusselt number, while the average $\langle Nu\rangle_\phi$ is increased due to eccentricity of the isotherms. The axial distance over which increase in Nusselt number occurs in region 2 is the same distance over which the isotherms of the hot core are observed to move outwards. We shall use these physical arguments to develop proper scalings for characteristic lengths and average Nusselt numbers for the first two regions.

NUSSELT NUMBER AND ENTRANCE LENGTH

The four regions in Fig. 1 are governed by different balances between advection and transverse diffusion. For purposes of scaling we will utilize the fully developed flow field of Mori and Nakayama [8], which is valid in the limit of small curvature and large Dean number, $De = Re\,\delta^{1/2}$. The

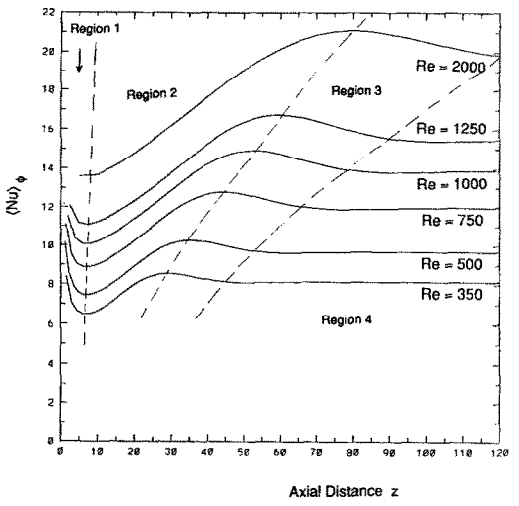

FIG. 1. Peripherally averaged Nusselt numbers in the thermal entrance region, $Pr = 1$, $\delta = 0.1$.

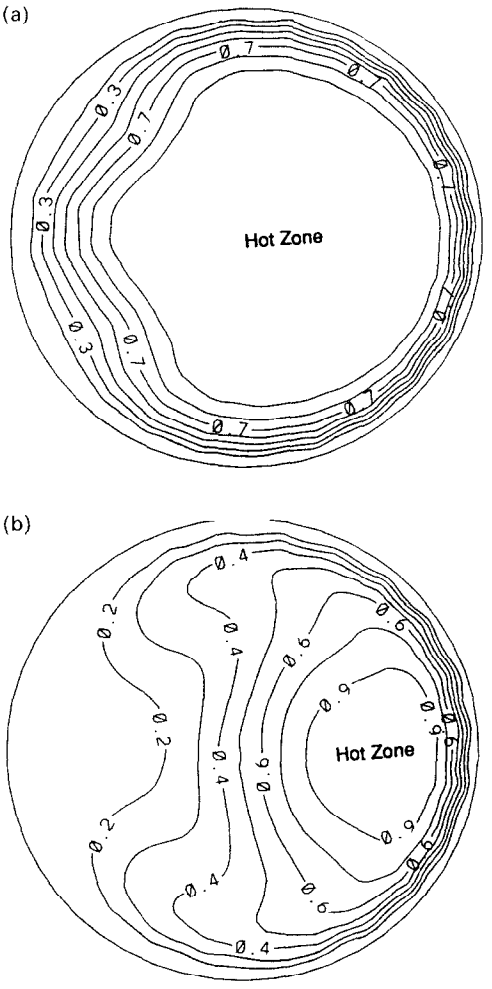

FIG. 2. Isotherms in the transverse plane for (a) $Re = 750$, $\delta = 0.1$ at $z = 5$, (b) $Re = 750$, $\delta = 0.1$ at $z = 25$.

dimensionless velocity components scale as $u \sim \delta^{1.4} Re^{-1.2}$, $v \sim \delta^{1.2}$, $w \sim O(1)$, where u is the radial velocity of the core flow in the cross-sectional plane, v the azimuthal velocity in the boundary layer, and w the mean axial velocity. Axial velocity in the boundary layer close to the tube wall, w_{bl}, scales as $w_{bl} \sim (1-r)(1+\cos\phi)De^{1/2}$.

Region 1

For Peclet number $Pe = Re\,Pr \gg 1$, the temperature field is everywhere uniform immediately following entry except close to the tube wall where a thermal boundary layer develops. In this region, axial advection balances radial diffusion so that

$$w\frac{\partial T}{\partial z} \sim \frac{1}{Pe}\frac{\partial^2 T}{\partial r^2}. \tag{1}$$

From this we get an estimation of the thermal boundary layer thickness

$$\delta_{to} \sim \left\{\frac{z}{Pe\,De^{1/2}}\frac{1}{1+\cos\phi}\right\}^{1/3} \tag{2}$$

valid for Pr around unity. The local Nusselt number is $1/\delta_{to}$ and its average over ϕ is given by

$$\langle Nu\rangle_\phi \sim De^{1/6}\left(\frac{Pe}{z}\right)^{1/3}. \tag{3}$$

For a short distance near the entrance, Nusselt number variation with axial distance shows an enhancement of $De^{1/6}$ as compared to that in straight tubes. This agrees with results reported by Dravid *et al.* [1].

Region 2

The second region begins when the thermal boundary layer thickness is of the same order as the eccentricity of the isotherms. This happens at $z = z_{min}$ which corresponds to the first minimum in the curves in Fig. 1. The displacement of a particle initially located at the center of the inlet section is $\varepsilon \sim z\delta^{1.4} Re^{-1.2}$, which gives an estimate of the eccentricity of the isotherms. Equating this to δ_{to} we get $z_{min} \sim \delta^{-1.2} Pr^{-1.2}$. There is also a weak Reynolds number dependence of z_{min} due perhaps to the neglected higher order terms in our scaling arguments. The following correlation is obtained from numerical data

$$z_{min} = 3.32 + 0.204 Re^{1.4}\delta^{1.2} Pr^{1.2}. \tag{4}$$

Comparison between this and numerical computations of z_{min} is shown in Fig. 3 for a variety of flow and geometrical parameters.

For $z > z_{min}$, radial advection affects the axial growth of the thermal boundary layer. Secondary flow increases the thermal boundary layer thickness δ_t on one side and decreases it on the other. To leading order we can set $\delta_t \approx \delta_{to}(1+\varepsilon\cos\phi)$. Since the local Nusselt number is $1/\delta_t$, we can obtain $\langle Nu\rangle_\phi$ by averaging over ϕ. To $O(\varepsilon^2)$, we get

$$\langle Nu\rangle_\phi \sim De^{1/6}\left(\frac{Pe}{z}\right)^{1/3}\left\{1+\tfrac{1}{2}z^2\delta^{1.2}Re^{-1.2}\right\} \tag{5}$$

which reduces to equation (3) for small z and concentric isotherms.

The order of magnitude estimates for regions 1 and 2 suggest that for small z, correlations can be obtained by considering $\langle Nu\rangle_\phi z^{1/3} De^{-1/6} Pe^{-1/3}$ as a function of $z\delta^{1.4} Re^{-1.2}$. Thus from numerical data we get

$$\langle Nu\rangle_\phi = 0.66 De^{1/6}\left(\frac{Pe}{z}\right)^{1/3}\left\{1+5.74\frac{z^2\delta^{1.2}}{Re}\right\}$$

$$\text{for } 0.07 < z\delta^{1.4}Re^{-1.2} \leqslant 0.3. \tag{6}$$

But for larger z the thermal boundary layer thickness estimate and the small ε assumption are not valid. The numerical data correlate with

$$\langle Nu\rangle_\phi = \left(\frac{Pe}{z}\right)^{1/2}\left\{0.86+1.03z\delta^{1.4}Re^{-1.2}\right\}^{1/2}$$

$$\text{for } 0.3 < z\delta^{1.4}Re^{-1.2} \leqslant 1. \tag{7}$$

Figure 4 shows these correlations compared to numerical data.

Regions 3 *and* 4

Equation (7) becomes invalid for $\varepsilon = z\delta^{1.4} Re^{-1.2}$ of order one when the hot core reaches the wall. Isotherms obtained numerically show that the transverse motion of the hot-fluid core is retarded at a radial location corresponding to $\varepsilon \approx 0.8$ due to the finite size of the core. This part of the $\langle Nu\rangle_\phi$ vs z data in Fig. 1 can be made to collapse on replotting it as $\langle Nu\rangle_\phi$ vs $z\delta^{1.4} Re^{-1.2}$. The Nusselt number begins to decrease again at $z_{max}\delta^{1.4} Re^{-1.2} \approx 0.85$. Thus z_{max} is approximately the axial distance required for fluid to move from the tube center to the wall.

The entrance length z_e is defined as the distance to the onset of the fully developed region 4. It is found to be approximately twice z_{max}. This distance corresponds to a fluid particle traversing the diametral distance from wall to wall along the plane of curvature. Actually, numerical results

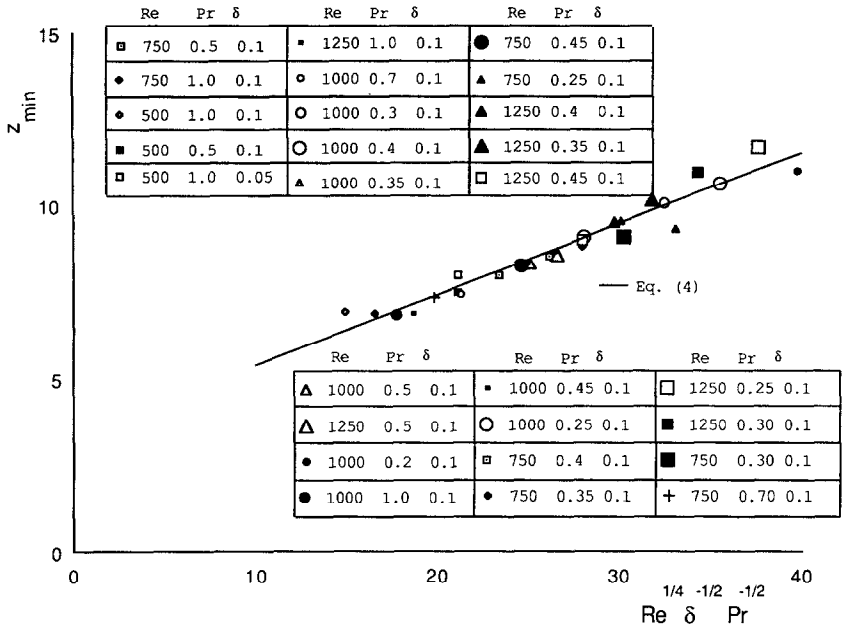

FIG. 3. Location of minimum Nusselt number.

indicate that this entrance length is a function of the Prandtl number also. For fluids with $Pr > 1$, the Nusselt number curve exhibits more than one oscillation corresponding to the number of transverse circulations required before the fully developed value is attained. The estimates provided here are expected to hold only for Pr around unity.

CONCLUSIONS

We have investigated the physical reasons for non-monotonic behavior of the peripherally averaged Nusselt number near the entrance of a coiled tube at high Peclet numbers. Four Nusselt number regions are evident. In region 1, heat transfer is dominated by thermal diffusion from the wall. In region 2 secondary flow in the transverse section distorts the axisymmetric development of the thermal boundary layer at the wall and increases the Nusselt number. Proper scaling provides estimates of locations at which the Nusselt number shows minima and maxima, as well as Nusselt number correlations for regions 1 and 2. When the hot core reaches the wall and begins to move inwards, the Nusselt number decreases again and approaches an asymptotic value downstream. This is in regions 3 and 4 which have not been modeled in detail.

Acknowledgement—This project was carried out under a Gas Research Institute Grant No. 5090-260-1971 monitored by Dr. Ferol Fish.

REFERENCES

1. A. N. Dravid, K. A. Smith, E. W. Merrill and P. L. T. Brian, Effect of secondary fluid motion on laminar flow

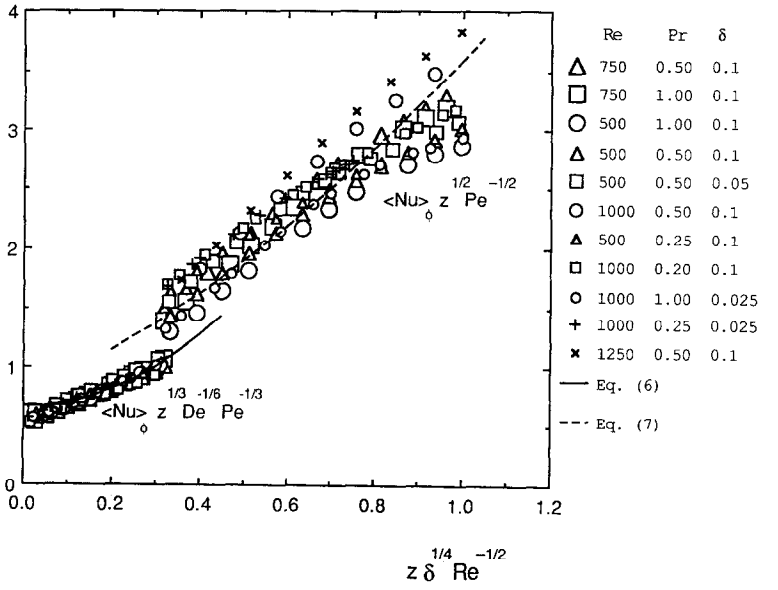

FIG. 4. Nusselt number correlations.

heat transfer in helically coiled tubes, *A.I.Ch.E. Jl* **17**, 1114–1122 (1971).
2. J. M. Tarbell and M. R. Samuels, Momentum and heat transfer in helical coils, *Chem. Engng J.* **5**, 117–127 (1973).
3. S. V. Patankar, V. S. Pratap and D. B. Spalding, Prediction of laminar flow and heat transfer in helically coiled pipes, *J. Fluid Mech.* **62**, 539–551 (1974).
4. M. Akiyama and K. C. Cheng, Laminar forced convection in the thermal entrance region of curved pipes with uniform wall temperature, *Can. J. Chem. Engng* **52**, 234–240 (1974).
5. L. A. M. Janssen and C. J. Hoogendoorn, Laminar convective heat transfer in helical coiled tubes, *Int. J. Heat Mass Transfer* **21**, 1197–1206 (1978).
6. N. Acharya, Experimental and numerical investigation of heat transfer enhancement in coiled tubes by chaotic mixing, Ph.D. Dissertation, University of Notre Dame, Notre Dame, Indiana (1992).
7. F. P. Incropera and D. P. DeWitt, *Fundamentals of Heat and Mass Transfer* (3rd Edn), p. 181. Wiley, New York (1990).
8. Y. Mori and W. Nakayama, Study on forced convective heat transfer in curved pipes (1st report, Laminar region), *Int. J. Heat Mass Transfer* **8**, 67–82 (1965).

Int. J. Heat Mass Transfer. Vol. 37, No. 2, pp. 340–343, 1994
Printed in Great Britain

0017-9310/94 $6.00 + 0.00

Effect of wall conduction on melting in an enclosure heated at constant rate

YUWEN ZHANG and ZHONGQI CHEN
Department of Power Machinery Engineering, Xi'an Jiaotong University, Xi'an 710049, China

(*Received* 21 *May* 1993 *and in final form* 8 *July* 1993)

1. INTRODUCTION

SOLID–LIQUID phase change phenomena exist widely in nature and industrial processes such as freezing of water and melting of ice, thermal energy storage, casting and metallurgical process, cryogenic preservation of blood and biomaterials, etc. Many typical applications of heat transfer in phase change involve convection in the liquid phase [1]. Recently, boundary layer theory has been adopted to solve the process of natural convection dominated melting. For example, the analytical solution for the melting process in a rectangular enclosure isothermally heated from one of its vertical walls was obtained by Bejan [2].

A series of laboratory experimental results and a compact boundary layer analysis were reported by Zhang and Bejan [3]. In their experiments, the wall heated at constant rate is made of aluminum and heated by eight uniformly spaced strip heaters. The temperature distribution along the two differentially heated vertical walls was measured by means of thermocouples positioned at four altitudes in the vertical mid-plane of the apparatus, and one of their typical measured wall temperatures is quoted in Fig. 1. In their theoretical analysis, the longitudinal conduction along the heated wall was not taken into account, this led to the 100% overprediction of the temperature gradient along the heated wall in the convection regime as illustrated in Fig. 4.

2. PHYSICAL MODEL AND MATHEMATICAL FORMULATION

The physical model adopted is shown as Fig. 2. The heated wall is made of aluminum with thickness w. The wall temperature is uniform as indicated in ref. [3] and rises linearly with time, which corresponds to the melting regime that is ruled by pure conduction; and then reaches a plateau in the convection melting regime. Quasi-steady state is said to be reached after the wall temperatures remain unchanged, all the heat supplied then is used to melt the solid phase change material (*n*-octadecane was used in ref. [3]). We assume that quasi-steady state is reached; the initial temperature of the solid phase in the enclosure is uniform and equal to the melting point T_m, i.e. no subcooling exists. The equations of the cold boundary layer, warm boundary layer and the core region and their corresponding boundary conditions were reported by Zhang and Bejan as follows [2, 3].

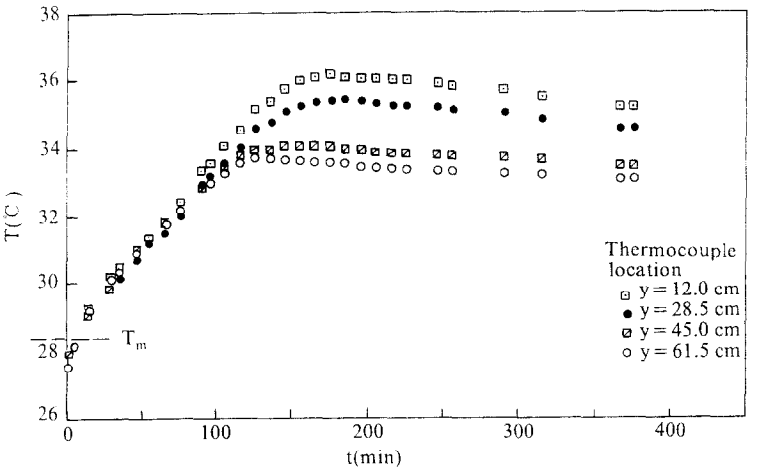

FIG. 1. The history of the temperature distribution along the heated plate [3].